JOURNAL OF GEOPHYSICAL RESEARCH, VOL. 104, NO. B12, PAGES 28,829–28,840, DECEMBER 10, 1999

Applicability of higher-order ray theory for *S* wave propagation in inhomogeneous weakly anisotropic elastic media

Václav Vavryčuk

Geophysical Institute, Academy of Sciences of the Czech Republic, Prague

Abstract. Modeling of *S* waves propagating in inhomogeneous, weakly anisotropic, elastic media creates complications for the zeroth-order ray theory. These complications are caused mainly by the so-called *S* wave coupling. If the *S* wave coupling is significant in the wave field, then the zeroth-order ray theory is inapplicable. In this case, modifications of the zeroth-order ray theory such as the coupling ray theory or the quasi-isotropic ray theory have so far been used to reproduce the *S* waves correctly. We show that the failure of the zeroth-order ray theory can also be overcome by higher-order ray theory. If we consider not only the zeroth-order term of the ray series but also higher-order terms, we can obtain correct results. On a simple example of a plane *S* wave propagating in a weak transversely isotropic medium with a rotating axis of symmetry, we study how the accuracy of higher-order ray theory depends on the number of higher-order ray approximations considered in the solution.

1. Introduction

Recently, several authors demonstrated difficulties of the zeroth-order ray theory (ZRT) when modeling *S* waves propagating in inhomogeneous, weakly anisotropic, elastic media [*Chapman and Shearer*, 1989; *Coates and Chapman*, 1990; *Guest et al.*, 1992; *Thomson et al.*, 1992]. These complications arise due to the interaction of split *S* waves, called "*S* wave coupling." The *S* wave coupling can be quite remarkable, when polarization vectors of the split *S* waves change rapidly along a ray (e.g., near *S* wave singularities), and the anisotropy of the medium is weak. Then the *S* wave coupling significantly affects the split *S* waves, and ZRT can only approximate a true solution very roughly, or it can even yield quite erroneous results. Moreover, the zeroth-order ray solution for an anisotropic medium may not necessarily converge to the zeroth-order ray solution for an isotropic medium, when anisotropy diminishes to isotropy. We can illustrate this surprising and very unwelcome property of ZRT on propagation of *S* waves in a one-dimensional (1-D) inhomogeneous anisotropic medium previously studied by *Lakhtakia* [1994] and by *Rümpker and Silver* [1998]. We shall assume a vertically inhomogeneous, transversely isotropic medium, where the inhomogeneity is caused by the symmetry axis of the medium rotating around the vertical axis (see Figure 1). If a plane *S* wave propagates in the vertical direction, ZRT predicts that the polarization of the *S* wave rotates coincidently with the rotation of the symmetry axis (see Figure 2). The rotation of the *S* wave polarization is independent of the strength of the anisotropy of the medium. Therefore, when we gradually diminish anisotropy to isotropy, ZRT always predicts the rotating *S* wave polarization as the wave propagates along the *z* axis. This is obviously an unphysical result, which contradicts the results of ray theory for an isotropic medium. The "isotropic" ray theory predicts constant *S* wave polarization, since the above mentioned medium becomes homogeneous when anisotropy vanishes (see Figure 2). We shall refer to this phenomenon as the "failure of ZRT." An analogous failure of ray theory can also occur in a strongly anisotropic medium, when the *S* wave propagates near the *S* wave singularity direction. In this case, the *S* wave coupling is also remarkable, and ZRT yields contradictory results. Thus ZRT can fail in weakly as well as in strongly anisotropic media, in the latter case, specifically for the directions near the *S* wave singularities.

Chapman and Shearer [1989] proposed to overcome the difficulties of ZRT by developing the *S* wave coupling theory valid for 1-D inhomogeneous anisotropic media. This method eliminates the failure of ZRT by incorporating the *S* wave coupling into the solution. *Coates and Chapman* [1990] modified the above mentioned approach and developed an extension of asymptotic ray theory valid for 3-D inhomogeneous anisotropic media called the coupling ray theory. *Sharafutdinov* [1994], *Pšenčík* [1998], and *Zillmer et al.* [1998] use an another modification of ZRT called the quasi-isotropic approximation. This method again takes into account the *S* wave coupling to obtain correct results for *S* wave propagation in inhomogeneous weakly anisotropic media. All these modifications of ray theory eliminate the failure of ZRT, and their results converge smoothly to the ray results for isotropic media when anisotropy diminishes to isotropy.

In this paper we propose another ray-based approach for studying *S* waves propagating in inhomogeneous anisotropic media, called higher-order ray theory (HRT). We suggest consideration of not only the zeroth-order term of the ray series but also higher-order terms [*Vavryčuk and Yomogida*, 1996; *Vavryčuk*, 1997]. Using this approach, we shall solve the problem of propagation of the plane *S* wave in the weakly transversely isotropic medium with a rotating axis of symmetry. We shall simplify the problem to be able to calculate the ray solution analytically. By applying first-order perturbation theory we shall express explicitly formulae for all higher-order ray approximations and thus obtain the

Paper number 1999JB900296.
0148-0227/99/1999JB900296$09.00

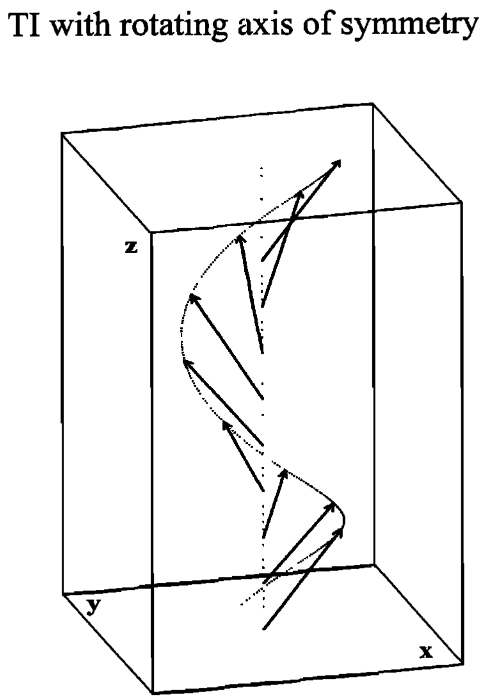

Figure 1. Vertically inhomogeneous transversely isotropic medium. Direction of the symmetry axis depends on the z coordinate and rotates around the z axis.

complete ray solution. We shall illustrate that the failure of ZRT can be removed by HRT, and that the S wave coupling ignored by ZRT can be reproduced well by HRT. Using numerical examples, we shall study the accuracy of the ray solution by comparing the ray solution with the exact solution obtained by the finite difference (FD) method. The accuracy of the ray solution will be studied via its dependence on the number of higher-order ray terms, on the strength of anisotropy, and on the strength of inhomogeneity, meaning the rate of rotation of the symmetry axis of the medium along the z axis.

2. Ray Theory for Inhomogeneous Anisotropic Media

The elastodynamic equation for an inhomogeneous, anisotropic, elastic medium, when no sources are considered, reads

$$\rho \ddot{u}_i - \left(\rho\, a_{ijkl}\, u_{k,l}\right)_{,j} = 0\,, \quad i = 1,2,3, \tag{1}$$

where $\mathbf{u} = \mathbf{u}(\mathbf{x}, t)$ is the displacement, ρ is the density of the medium, a_{ijkl} are the density-normalized elastic parameters, and t is time. We assume that elastic parameters a_{ijkl} and density ρ and their derivatives are continuous functions of coordinates. Solving (1) using ray theory, we seek a solution in the form of the ray series [*Červený*, 1972, equation 3; *Červený et al.*, 1977, equation 5.2]

$$u_i(\mathbf{x}, t) = \sum_{K=0}^{\infty} U_i^{(K)}(\mathbf{x})\, f^{(K)}\left(t - \tau(\mathbf{x})\right), \tag{2}$$

where

$$\frac{d}{dt} f^{(K)}(t) = f^{(K-1)}(t)\ .$$

K denotes the order of the ray approximation, $\mathbf{U}^{(K)}(\mathbf{x})$ is the ray amplitude vector, and $\tau(\mathbf{x})$ is the travel time. Equation (2) describes the ray expansion of only one wave. Since P, $S1$, or $S2$ waves can propagate in anisotropic media, we have to sum the ray expansions of these three waves. If we consider only the first term of the ray expansion (2), we shall speak of the ZRT solution. If we sum the higher-order terms ($K = 1,\ldots,\infty$) in equation (2), we shall speak of the complete HRT solution. The complete ray solution is then a sum of the ZRT and HRT solutions.

Inserting (2) into (1) leads to the system of basic equations of ray theory for the ray amplitudes $\mathbf{U}^{(K)}$:

$$N_i(\mathbf{U}^{(K)}) - M_i(\mathbf{U}^{(K-1)}) + L_i(\mathbf{U}^{(K-2)}) = 0\ , \tag{3}$$

where **N**, **M**, and **L** are differential operators defined as [*Červený*, 1972, equation 6]

$$N_j\left(\mathbf{U}^{(K)}\right) = \Gamma_{jk} U_k^{(K)} - U_j^{(K)},$$

$$M_j\left(\mathbf{U}^{(K)}\right) = a_{ijkl}\, p_i \frac{\partial U_k^{(K)}}{\partial x_l} + \frac{1}{\rho}\frac{\partial}{\partial x_i}\left(\rho\, a_{ijkl}\, p_l U_k^{(K)}\right), \tag{4}$$

$$L_j\left(\mathbf{U}^{(K)}\right) = \frac{1}{\rho}\frac{\partial}{\partial x_i}\left(\rho\, a_{ijkl} \frac{\partial U_k^{(K)}}{\partial x_l}\right),$$

where

$$\Gamma_{jk} = a_{ijkl}\, p_i p_l\,, \qquad p_i = \frac{\partial \tau}{\partial x_i}\ .$$

$\mathbf{\Gamma}$ is the Christoffel tensor and $\mathbf{p}$ is the slowness vector. Solving (3), we obtain the ray amplitude $\mathbf{U}^{(K)}$ as the sum of the additional component $\mathbf{U}^{(K)\perp}$ and the principal component $\mathbf{U}^{(K)\parallel}$:

$$\mathbf{U}^{(K)} = \mathbf{U}^{(K)\perp} + \mathbf{U}^{(K)\parallel}\ , \tag{5}$$

which can be calculated from the system of recursive equations. For the $S1$ wave expansion we can put [*Červený*, 1972, equations 21, 22, and 29a,b]

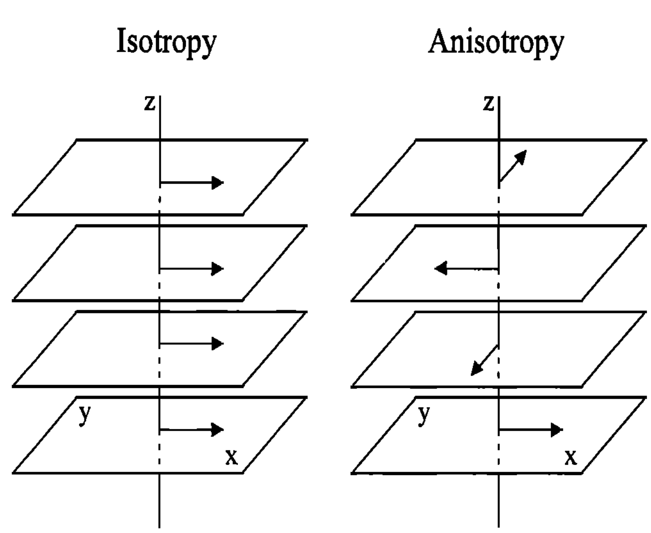

Figure 2. Ray theoretical polarizations of a plane S wave propagating along the z axis (left) in a homogeneous isotropic medium and (right) in an anisotropic medium with a rotating axis of symmetry.

For $K < 0$

$$U_k^{S1(K)\perp} = U_k^{S1(K)\parallel} = 0 \ , \tag{6a}$$

For $K = 0$

$$U_k^{S1(0)\perp} = 0 \ , \tag{6b}$$

$$U_k^{S1(0)\parallel} = \frac{g_k^{S1}}{\sqrt{\rho v^{S1} J^{S1}}} \sqrt{\rho_0 v_0^{S1} J_0^{S1}}\, C^{S1(0)} \ , \tag{6c}$$

For $K > 0$

$$U_k^{S1(K)\perp} = \left[M_i(\mathbf{U}^{S1(K-1)}) - L_i(\mathbf{U}^{S1(K-2)}) \right] \times \left[\frac{g_i^{S2} g_k^{S2}}{G^{S2} - G^{S1}} + \frac{g_i^P g_k^P}{G^P - G^{S1}} \right] , \tag{6d}$$

$$U_k^{S1(K)\parallel} = \frac{g_k^{S1}}{\sqrt{\rho v^{S1} J^{S1}}} \left\{ \sqrt{\rho_0 v_0^{S1} J_0^{S1}}\, C^{S1(K)} + \frac{1}{2} \int_{s_0}^{s} \sqrt{\frac{\rho J^{S1}}{v^{S1}}} \left[L_i(\mathbf{U}^{S1(K-1)}) - M_i(\mathbf{U}^{S1(K)\perp}) \right] g_i^{S1} ds \right\} , \tag{6e}$$

where v is the group velocity, $\mathbf{g}$ is the polarization vector, G is the eigenvalue of the Christoffel tensor $\mathbf{\Gamma}$, s is the arc length of the ray, and $C^{(K)} = C^{(K)}(\gamma_1, \gamma_2)$ is the integration constant of the Kth-order ray approximation. The integration constant depends on ray parameters γ_1 and γ_2 and should be determined from the boundary conditions. J denotes the ray Jacobian, which is defined as the Jacobian of the transformation from the Cartesian coordinates x, y, z to the ray coordinates s, γ_1, and γ_2. Quantities with subscript zero are taken at the initial point of the ray; the other quantities are taken at the observation point.

Equation (6) is very general, valid for arbitrary wave fields in 3-D inhomogeneous anisotropic media. We only do not consider phase shifts due to caustics. Analogous equations can be written also for the P or $S2$ wave expansions.

3. Weak Transverse Isotropy With Rotating Axis of Symmetry

Let us consider transversely isotropic medium with a vertical axis of symmetry with the following density-normalized elastic parameters:

$$\mathbf{a} = \begin{bmatrix} a_{11} & a_{11} - 2a_{66} & a_{11} - 2a_{44} & 0 & 0 & 0 \\ & a_{11} & a_{11} - 2a_{44} & 0 & 0 & 0 \\ & & a_{11} & 0 & 0 & 0 \\ & & & a_{44} & 0 & 0 \\ & & & & a_{44} & 0 \\ & & & & & a_{66} \end{bmatrix} , \tag{7}$$

where the 2-index Voigt notation has been used. This medium represents a special type of transverse isotropy, which is very simple and in many aspects similar to isotropy. For example, polarization vectors of P, SV, and SH waves in the medium are identical to those in isotropic media. Also phase velocities of P and SV waves are constant and the same as for isotropic media

$$c^P = \sqrt{a_{11}} \ , \ c^{SV} = \sqrt{a_{44}} \ . \tag{8}$$

The only difference between this simple transverse isotropy and isotropy is that the phase velocity of the SH wave is directionally dependent having the following form:

$$c^{SH} = \sqrt{a_{66} \sin^2\theta + a_{44} \cos^2\theta} \ , \tag{9}$$

where θ is the angle between the phase normal and the symmetry axis. For the symmetry axis direction ($\theta = 0°$) the SV and SH waves have coincident phase velocities and form a kiss singularity [*Crampin*, 1991]. For other directions the SV and SH waves propagate with different phase velocities, thus splitting into two independent waves. If parameters a_{44} and a_{66} have similar values, $|a_{66} - a_{44}| << a_{44}$, the transverse isotropy becomes weak. Equation (9) can then be linearized as

$$c^{SH} = \sqrt{a_{44}} \left(1 + \gamma \sin^2\theta \right) \ , \tag{10a}$$

where

$$\gamma = \frac{a_{66} - a_{44}}{2a_{44}} \ , \quad |\gamma| << 1 \ . \tag{10b}$$

Parameter γ is the well-known *Thomsen* [1986, equation 8b] parameter, the other *Thomsen* [1986, equations 8a and 17] parameters ε and δ are zero in our case.

The above mentioned weakly transversely isotropic (WTI) medium will serve to construct the 1-D inhomogeneous anisotropic medium under study. First, we shall incline the symmetry axis of the WTI medium from the vertical by constant and nonzero angle ϑ. Second, the axis of symmetry will rotate uniformly around the vertical in dependence on the z coordinate (see Figure 1). Thus the unit direction vector of the symmetry axis will be expressed as

$$\mathbf{N}(z) = \begin{bmatrix} -\sin\vartheta \cos\varphi(z) \\ \sin\vartheta \sin\varphi(z) \\ \cos\vartheta \end{bmatrix} , \tag{11}$$

where ϑ is the deviation of the symmetry axis from the vertical, $\varphi = bz$ is the angle of rotation of the symmetry axis which is measured in the x-y plane, and b is the parameter expressing the rate of rotation. We assume b being constant and positive, $b > 0$.

In this way we obtain a vertically inhomogeneous WTI medium called the WTI medium with a rotating axis of symmetry. The expressions for the elastic parameters a'_{kl} of this medium are given in Appendix A. The density of the medium is constant.

4. Propagation of Plane *S* Waves Along the *z* Axis by Higher-Order Ray Theory

In this section we shall study the properties of plane S waves propagating in the above defined medium along the z axis by applying higher-order ray theory. The wave will propagate from $z = 0$ in the positive direction. At the initial point, $z = 0$, the S wave will be linearly polarized in the direction of the x axis and will have the form of the Dirac delta function in time. In ray theory the studied S wave is composed of two elementary S waves: SR (radial S) and ST (transverse S). Both S waves are polarized in the x-y plane. Polarization vector of the SR wave is parallel to the horizontal projection of the symmetry axis of WTI, and polarization vector of the ST wave is perpendicular to this projection (see

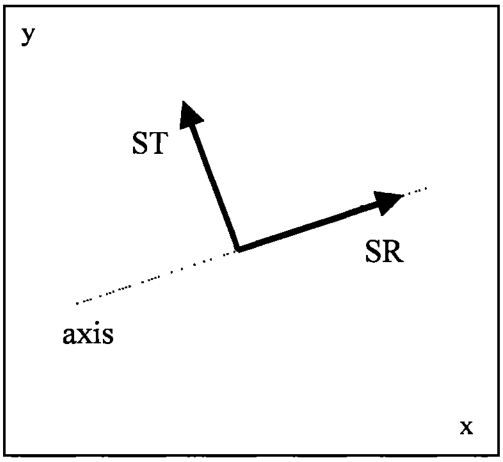

Figure 3. Definition of the *SR* and *ST* waves. Dotted line is projection of the symmetry axis of the medium into the *x-y* plane.

Figure 3). We shall now express analytically the basic ray quantities and, subsequently, the zeroth-order term and all the higher-order terms of the ray expansions of these waves.

4.1. Ray Fields and Ray Jacobians of the *SR* and *ST* Waves

Ray fields of the *SR* and *ST* waves are different. For the *SR* wave the ray field is very simple because the phase and group velocity vectors are independent of ray direction and, in fact, are constant. Therefore the rays are straight lines parallel to the phase normal, and the ray Jacobian is unity:

$$c^{SR} = v^{SR} = \sqrt{a_{44}}\ ,\ J^{SR} = 1\ , \qquad (12)$$

where c^{SR} and v^{SR} are the phase and group velocities of the *SR* wave and J^{SR} is the ray Jacobian.

For the *ST* wave the ray field is more complicated. Since the deviation between the phase normal and the symmetry axis of WTI is constant, $\vartheta = \text{const}$, the magnitude of the group velocity of the *ST* wave is also constant for all points on the ray. However, the group velocity direction depends on the symmetry axis direction that rotates along the *z* axis. This results in rays forming a circular helix (see Figure 4):

$$x = x_0 + r_0 \sin\varphi\ ,\ y = y_0 + r_0 \cos\varphi\ ,\ z = c^{ST} t = b^{-1}\varphi\ , \qquad (13)$$

where

$$r_0 = b^{-1} \sin\delta\ ,$$

where x_0 and y_0 are ray parameters, φ is the monotonically increasing angle of rotation of the symmetry axis of WTI, b is the rate of rotation, c^{ST} is the phase velocity of the *ST* wave, and δ is the angle between the *z* axis and the ray. Phase and group velocities c^{ST} and v^{ST} and deviation δ can be approximately expressed in WTI as follows:

$$c^{ST} = v^{ST} = \sqrt{a_{44}}\left(1 + \gamma \sin^2\vartheta\right),\ \sin\delta = 2\gamma \sin\vartheta \cos\vartheta\ , \qquad (14)$$

where γ is the Thomsen parameter defined by (10b) and ϑ is the angle between the *z* axis and the symmetry axis of WTI. Similar to the *SR* wave, the ray Jacobian is constant and unity,

$$J^{ST} = 1\ . \qquad (15)$$

We emphasize that contrary to the *SR* wave where (12) holds exactly, (14) and (15) for the *ST* wave are approximate, being valid only under a weak anisotropy condition. For strong anisotropy, phase and group velocities c^{ST} and v^{ST} differ, and ray Jacobian J^{ST} is different from unity.

4.2. Zeroth- and Higher-Order Ray Approximations

Since the *S* wave has the form of the Dirac delta function at $z = 0$, we can express time functions $f^{(K)}(t)$ in (2) as follows:

$$f^{(0)}(t) = \delta(t),\ f^{(K)}(t) = \frac{t^{K-1}}{(K-1)!} H(t),\ K > 0\ . \qquad (16)$$

Taking into account (6), (12), and (15), we obtain for the zeroth-order ray approximation of the *SR* and *ST* waves

$$u_k^{SR(0)}(z,t) = C^{SR(0)} g_k^{SR} \delta\left(t - \frac{z}{c^{SR}}\right), \qquad (17a)$$

$$u_k^{ST(0)}(z,t) = C^{ST(0)} g_k^{ST} \delta\left(t - \frac{z}{c^{ST}}\right), \qquad (17b)$$

where

$$\mathbf{g}^{SR} = \begin{bmatrix} \cos\varphi \\ -\sin\varphi \\ 0 \end{bmatrix},\ \mathbf{g}^{ST} = \begin{bmatrix} \sin\varphi \\ \cos\varphi \\ 0 \end{bmatrix},\ \varphi = bz\ . \qquad (17c)$$

We can see from (17) that polarization of the *SR* and *ST* waves rotates in coincidence with the rotation of the symmetry axis of WTI. This rotation is independent of the strength of the anisotropy controlled by the Thomsen parameter γ. The *K*th-order ray approximations for $K > 0$ read

$$u_k^{ST(K)}(z,t) = U_k^{ST(K)} \frac{\left(t - \tau^{ST}\right)^{K-1}}{(K-1)!} H\left(t - \tau^{ST}\right)\ , \qquad (18a)$$

$$u_k^{SR(K)}(z,t) = U_k^{SR(K)} \frac{\left(t - \tau^{SR}\right)^{K-1}}{(K-1)!} H\left(t - \tau^{SR}\right)\ . \qquad (18b)$$

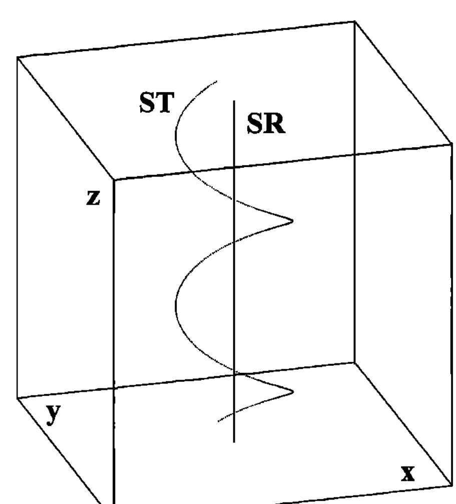

Figure 4. Geometry of rays of the *SR* and *ST* waves.

Using (17) and (18) for the zeroth- and higher-order terms of the ray expansion and (6) for ray amplitudes, we can recursively calculate the complete ray series for the *SR* and *ST* waves. Although the medium is very simple and we are studying the propagation of a plane wave, the procedure of analytical calculation of higher-order ray approximations involves extensive manipulation with rather complex formulae. Therefore we performed the calculations by using symbolic manipulation software REDUCE [*Hearn*, 1991]. In the sections 4.3-4.4, we shall not present a detailed derivation but only basic steps and the final formulae.

4.3. Integration Constants

The fundamental problem in calculating the higher-order ray approximations is to determine the zeroth- and higher-order integration constants. The integration constants should be determined from the boundary conditions imposed on the S wave at $z = 0$. Since the incident S wave has the form of the Dirac delta function polarized in the x axis,

$$\mathbf{u}^S(z=0,t) = (\delta(t),0,0)^T , \tag{19}$$

we conclude that

$$C^{SR(0)} = 1 , \quad C^{ST(0)} = 0 . \tag{20}$$

The higher-order integration constants of the *SR* and *ST* waves are determined from

$$\sum_{K=1}^{\infty} \left[\mathbf{u}^{SR(K)}(z=0,t) + \mathbf{u}^{ST(K)}(z=0,t)\right] = 0 , \tag{21}$$

expressing the fact that the higher-order ray approximations of the *SR* and *ST* waves cancel each other at $z = 0$. Obviously, if (20) and (21) are satisfied, the boundary conditions are also satisfied. Since travel times τ^{SR} and τ^{ST} are zero at $z = 0$, (18) and (21) yield

$$\sum_{K=1}^{\infty} \left[U^{SR(K)\parallel}(z=0) + U^{ST(K)\perp}(z=0)\right] t^{K-1} = 0 , \tag{22a}$$

$$\sum_{K=1}^{\infty} \left[U^{ST(K)\parallel}(z=0) + U^{SR(K)\perp}(z=0)\right] t^{K-1} = 0 . \tag{22b}$$

Equation (22) should be valid for all times t, and thus we can decompose it into a system of recursive equations for the higher-order integration constants:

$$U^{SR(K)\parallel}(z=0) + U^{ST(K)\perp}(z=0) = 0 , \tag{23a}$$

$$U^{ST(K)\parallel}(z=0) + U^{SR(K)\perp}(z=0) = 0 . \tag{23b}$$

Using (23), we can express the first-order integration constants as follows:

$$C^{ST(1)} = \left(\frac{\sqrt{a_{44}}\,b}{\gamma\sin^2\vartheta}\right)\left[1+\gamma\sin^2\vartheta\right] , \quad C^{SR(1)} = 0 , \tag{24a}$$

and the other higher-order integration constants as follows ($K > 0$):

$$C^{ST(2K)} = 0 , \tag{24b}$$

$$C^{SR(2K)} = \frac{(2K-1)!}{K!\,(K-1)!}\left(\frac{\sqrt{a_{44}}\,b}{\gamma\sin^2\vartheta}\right)^{2K}\left[1+3K\gamma\sin^2\vartheta\right] , \tag{24c}$$

$$C^{SR(2K+1)} = 0 , \tag{24d}$$

$$C^{ST(2K+1)} = \frac{2(2K-1)!}{K!\,(K-1)!}\left(\frac{\sqrt{a_{44}}\,b}{\gamma\sin^2\vartheta}\right)^{2K+1}\left[1+(3K+1)\gamma\sin^2\vartheta\right] . \tag{24e}$$

4.4. Complete Ray Solution

The final formulae for the *SR* and *ST* wave ray series are expressed as follows:

$$u_k^{ST}(z,t) = U_k^{ST(0)}\delta\left(t-\tau^{ST}\right) + \sum_{K=1}^{\infty} U_k^{ST(K)} \frac{\left(t-\tau^{ST}\right)^{K-1}}{(K-1)!} H\left(t-\tau^{ST}\right) , \tag{25a}$$

$$u_k^{SR}(z,t) = U_k^{SR(0)}\delta\left(t-\tau^{SR}\right) + \sum_{K=1}^{\infty} U_k^{SR(K)} \frac{\left(t-\tau^{SR}\right)^{K-1}}{(K-1)!} H\left(t-\tau^{SR}\right) . \tag{25b}$$

Ray amplitudes $\mathbf{U}^{SR(K)}$ and $\mathbf{U}^{ST(K)}$ read

$$U_k^{SR(K)} = U^{SR(K)\parallel} g_k^{SR} + U^{SR(K)\perp} g_k^{ST} , \tag{26a}$$

$$U_k^{ST(K)} = U^{ST(K)\parallel} g_k^{ST} + U^{ST(K)\perp} g_k^{SR} , \tag{26b}$$

For $K = 0$

$$U^{ST(0)\parallel} = U^{ST(0)\perp} = 0 , \; U^{SR(0)\parallel} = 1 , \; U^{SR(0)\perp} = 0 , \tag{26c}$$

For $K > 0$

$$U^{SR(K)\parallel} = \left(1+\frac{3}{2}K\gamma\sin^2\vartheta\right)\left(\frac{b\sqrt{a_{44}}}{\gamma\sin^2\vartheta}\right)^K (K-1)! \times \sum_{N=0}^{N\le\frac{K}{2}} \frac{\varphi^{K-2N}}{N!(K-N-1)!\,(K-2N)!} , \tag{26d}$$

$$U^{SR(K)\perp} = -\left(1+\frac{1}{2}(3K-1)\gamma\sin^2\vartheta\right)\left(\frac{b\sqrt{a_{44}}}{\gamma\sin^2\vartheta}\right)^K (K-1)! \times \sum_{N=0}^{N\le\frac{K-1}{2}} \frac{\varphi^{K-2N-1}}{N!(K-N-1)!\,(K-2N-1)!} , \tag{26e}$$

$$U^{ST(K)\parallel} = (-1)^{K-1}\left(1+\frac{1}{2}(3K-1)\gamma\sin^2\vartheta\right)\left(\frac{b\sqrt{a_{44}}}{\gamma\sin^2\vartheta}\right)^K (K-1)! \times \sum_{N=0}^{N\le\frac{K-1}{2}} \frac{\varphi^{K-2N-1}}{N!(K-N-1)!\,(K-2N-1)!} , \tag{26f}$$

$$U^{ST(K)\perp} = (-1)^{K-1}\left(1+\frac{3}{2}K\gamma\sin^2\vartheta\right)\left(\frac{b\sqrt{a_{44}}}{\gamma\sin^2\vartheta}\right)^K (K-1)! \times \sum_{N=0}^{N\le\frac{K-2}{2}} \frac{\varphi^{K-2N-2}}{N!(K-N-1)!\,(K-2N-2)!} . \tag{26g}$$

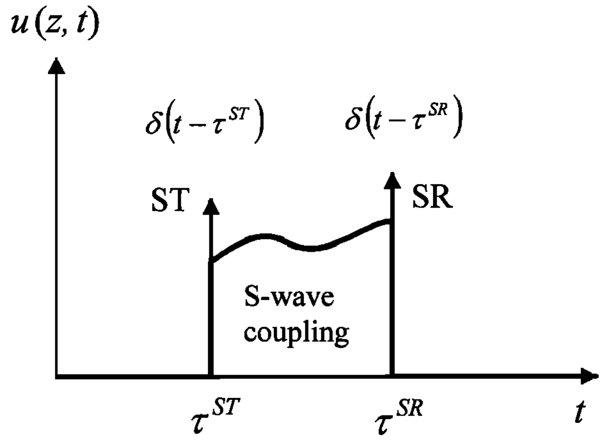

Figure 5. Schematic diagram of the ST and SR zeroth-order waves (with waveforms of the Dirac delta function) together with the S wave coupling (bold line).

where K is the order of the ray approximation, b is the rate of rotation of the symmetry axis ($b > 0$), ϑ is the angle between the symmetry axis and the z axis, anisotropy parameter γ is defined in (10b), $\varphi = bz$ is the angle of rotation, and $\mathbf{g}^{SR}$ and $\mathbf{g}^{ST}$ are unit polarization vectors defined in (17c). Travel times τ^{SR} and τ^{ST} in (25) are expressed as follows:

$$\tau^{SR} = \frac{z}{\sqrt{a_{44}}}\ , \quad \tau^{ST} = \frac{z}{\sqrt{a_{44}}}\left(1-\gamma\sin^2\vartheta\right) . \qquad (27)$$

Note that for infinitesimally weak anisotropy ($\gamma \to 0$), ray amplitudes in (26) diverge. It is caused by the denominator $G^{SR} - G^{ST}$ in (6d), which is proportional to γ. Although the ray amplitudes diverge for $\gamma \to 0$, the complete ray solution (25) can converge and thus can yield the true solution. It converges, namely, in the time interval defined by arrivals of ST and SR zeroth-order waves, where the S wave coupling can occur [see *Chapman and Shearer*, 1989]. Therefore we apply (25) only for this time interval. For the other times, we simply put the solution being zero (see Figure 5).

Note that (25) and (26) are valid for the S wave propagating not only in a weakly anisotropic medium but also in a strongly anisotropic medium supposing that angle ϑ between the symmetry axis and the z axis is small. In fact, the term, which should be small in (26), is $\gamma\sin^2\vartheta$. This term vanishes either for $\gamma \to 0$ or for $\vartheta \to 0$. The latter case corresponds to the strongly anisotropic medium, in which the plane S wave propagates near the S wave singularity.

4.5. Limit From Anisotropy to Isotropy

If the anisotropy is very weak, the higher-order ray amplitudes (26) become very high, but they are concentrated in a very narrow time interval (see Figure 6). For vanishing anisotropy ($\gamma \to 0$) the ray amplitudes diverge, but the width of the time interval vanishes. Hence the waveform of the HRT solution becomes the Dirac delta function similarly to the ZRT solution. Thus the complete ray solution in the limit from anisotropy to isotropy can be expressed as

$$\mathbf{u}^{iso}(z,t) \equiv \lim_{\gamma\to 0}\mathbf{u}(z,t) = \mathbf{U}^{iso}(z)\,\delta\left(t-\frac{z}{\sqrt{a_{44}}}\right) , \qquad (28)$$

where amplitude $\mathbf{U}^{iso}(z)$ is calculated as the sum of the zeroth-order ray amplitude and the time integral of the HRT solution of the faster S wave over the time interval between the SR and ST wave arrivals (see Figure 6, hatched area). If anisotropy parameter γ is positive, the faster wave is the ST wave and amplitude $\mathbf{U}^{iso}(z)$ can be expressed as follows:

$$\mathbf{U}^{iso}(z) = \mathbf{g}^{SR} + \lim_{\gamma\to 0}\int_{\tau^{ST}}^{\tau^{SR}} \mathbf{u}^{ST}(z,t)\,dt = \mathbf{g}^{SR}$$

$$+ \lim_{\gamma\to 0}\sum_{K=1}^{\infty}\left[\left(\mathbf{g}^{ST}U^{ST(K)\parallel} + \mathbf{g}^{SR}U^{ST(K)\perp}\right)\frac{1}{(K-1)!}\int_{\tau^{ST}}^{\tau^{SR}}\left(t-\tau^{ST}\right)^{K-1}dt\right]$$

$$= \mathbf{g}^{ST}\lim_{\gamma\to 0}\sum_{K=1}^{\infty}\left[\frac{1}{K!}U^{ST(K)\parallel}\left(\tau^{SR}-\tau^{ST}\right)^{K}\right]$$

$$+\mathbf{g}^{SR}\left\{1+\lim_{\gamma\to 0}\sum_{K=1}^{\infty}\left[\frac{1}{K!}U^{ST(K)\perp}\left(\tau^{SR}-\tau^{ST}\right)^{K}\right]\right\} . \qquad (29)$$

Taking into account that

$$\tau^{SR} - \tau^{ST} = \frac{\gamma\sin^2\vartheta}{b\sqrt{a_{44}}}\varphi \qquad (30)$$

and using (26), we obtain

$$\lim_{\gamma\to 0}\sum_{K=1}^{\infty}\left\{\frac{1}{K!}U^{ST(K)\parallel}\left(\tau^{SR}-\tau^{ST}\right)^{K}\right\} = \sum_{K=0}^{\infty}(-1)^K\frac{\varphi^{2K+1}}{(2K+1)!} = \sin\varphi , \qquad (31a)$$

$$1+\lim_{\gamma\to 0}\sum_{K=1}^{\infty}\left\{\frac{1}{K!}U^{ST(K)\perp}\left(\tau^{SR}-\tau^{ST}\right)^{K}\right\} = \sum_{K=0}^{\infty}(-1)^K\frac{\varphi^{2K}}{(2K)!} = \cos\varphi . \qquad (31b)$$

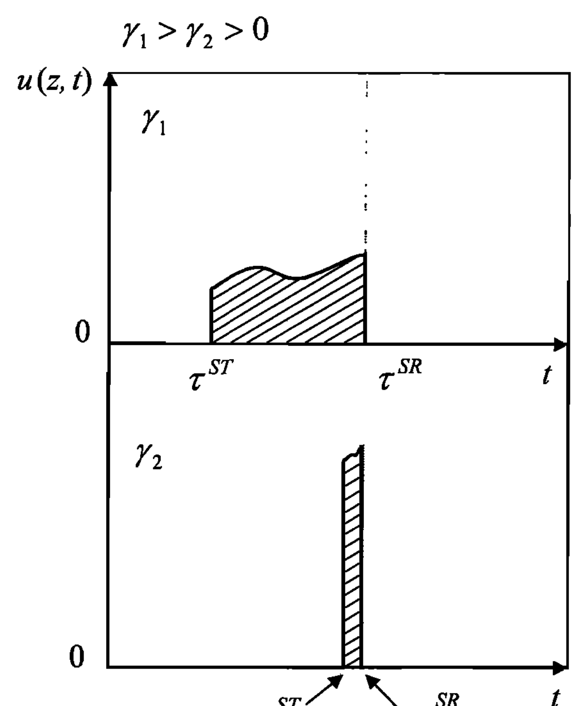

Figure 6. Schematic diagram of two HRT solutions at the same observation point but for different anisotropy models descibed by parameters γ_1 and γ_2: $\gamma_1 > \gamma_2 > 0$. Travel time τ^{SR} is independent of γ.

Thus

$$\mathbf{U}^{iso}(z, t) = (1, 0, 0)^T$$

and the final formula for the complete ray solution in the isotropic limit $\mathbf{u}^{iso}(z, t)$ is expressed as follows:

$$\mathbf{u}^{iso}(z, t) = (1, 0, 0)^T \delta\left(t - \frac{z}{\sqrt{a_{44}}}\right). \quad (32)$$

Obviously, we found a true solution. In a homogeneous isotropic medium the plane S wave propagates with a constant amplitude and is polarized identically as the incident S wave independently of the z coordinate. A similar result is obtained for a negative anisotropy parameter γ, when the faster wave is the SR wave.

5. Numerical Example

In this section we shall give a numerical example of applying the ray theoretical formulae derived in section 4. We shall calculate the ray solution for a number of higher-order ray approximations and compare with the reference solution called also the exact solution and obtained by the finite difference (FD) method described in Appendix B.

Accordingly to section 4 we shall assume that the incident plane S wave is polarized at $z = 0$ along the x axis and thus being the pure SR wave at $z = 0$. The incident S wave will have a unit amplitude, and the waveform will be a one-sided pulse expressed as

$$\mathbf{u}(z = 0, t) = \left[\sin^2\left(\frac{\pi t}{T}\right), 0, 0\right]^T \quad \text{for } t \in < 0, T > . \quad (33)$$

For other times, $\mathbf{u}(z = 0, t)$ will be zero. For pulse width T we use the value $T = 1$ s.

The S wave will propagate in two medium models. The first model is called the "weak anisotropy" model and is specified by values $a_{44} = 6.00$ and $\gamma = 0.15$. The second model is called the "very weak anisotropy" model being specified by values $a_{44} = 6.00$ and $\gamma = 0.003$. The ST wave anisotropy (defined as the directional variation of the ST wave phase velocity) attains 13% for the weak anisotropy model and 0.3% for the very weak anisotropy model. The latter model displays 50 times weaker anisotropy than the first model, thus almost approaching isotropy. Note that we do not need to specify parameter a_{11} for the S wave propagation. The symmetry axis deviates from the z axis by angle $\vartheta = 60°$. For the rate of rotation of the symmetry axis we use values b = 0.032, 0.064, 0.096, and 0.128, which correspond to the rotation of the symmetry axis through angle $\varphi = \pi$ over distances $z = 40\lambda^{SR}$, $20\lambda^{SR}$, $13.3\lambda^{SR}$, and $10\lambda^{SR}$, where λ^{SR} denotes the wavelength of the incident S wave, $\lambda^{SR} = c^{SR}T = \sqrt{a_{44}}\,T = 2.45$ km.

The propagating S wave will be calculated using the ray method by (25)-(26) and using the FD method by (B5). In the FD calculations we have used the following values of the space and time steps: $\Delta z = 0.02$ km and $\Delta t = 0.004$ s.

Figure 7 shows a comparison of the ZRT solution with the exact solution for four receivers in the weak and very weak anisotropy models. We can see from the left-hand diagrams that the incident S wave is polarized at $z = 0$ along the x axis, thus being the pure SR wave. As the wave propagates through the medium, the exact waveforms and particle motions (Figure 7, solid line) change. The changes are more distinct for weak anisotropy than for very weak anisotropy. In very weak anisotropy the predominant S wave polarization remains unchanged, and the quasi-ellipticity of the wave increases only slightly. In weak anisotropy, however, the quasi-ellipticity of the S wave is approximately constant, but the predominant polarization direction rotates in coincidence with the rotation of the symmetry axis of the medium. For the most distant receiver (right-hand diagrams) we observe the forming of an another S wave, which is faster having a smaller amplitude and being polarized perpendicularly to the polarization of the predominant and slower S wave.

For both anisotropy models, ZRT predicts the same results (Figure 7, dashed line): the propagating S wave is a pure SR wave for all receivers, it is linearly polarized, and it has a unit amplitude. In the weak anisotropy model, polarization of the ZRT wave coincides with the predominant polarization direction of the exact S wave. In the very weak anisotropy model, however, the waveforms and particle motions of the ZRT solution are distinctly different from the exact solution. Therefore ZRT fails totally in this case. However, if we include 10 higher-order ray approximations, we obtain a result identical with the exact solution (Figure 7, solid line). Hence ZRT fails, but HRT yields correct results.

Figure 8 shows the behavior of the ray solution when a different number of higher-order ray approximations is considered. Waveforms and particle motions are shown for the receiver at $z = 13.3\lambda^{SR}$. For both anisotropy models the fit between the exact and ray solutions improves rapidly if the higher-order ray approximations are included. The more approximations we consider, the better fit we obtain. For the configuration used, the six higher-order ray approximations are sufficient to reproduce the exact solution within the width of the line.

Figure 9 displays the comparison of the exact and ray solutions for anisotropy models with a different rate of rotation of the symmetry axis. The waveforms and particle motions are displayed for the receiver at $z = 6.6\lambda^{SR}$. The rate of the symmetry axis rotation increases in the diagrams from left to right. Comparing the diagrams with the different rates of rotation, we observe that the fit between the exact and ray solutions decreases with increasing rate of rotation. Therefore, for higher rates of rotation we have to consider a higher number of ray approximations to obtain a solution of reasonable accuracy. Specifically, for the rate of rotation $b = \pi / 10\,\lambda^{SR}$ the differences between the exact solution and the ray solution with seven higher-order ray approximations are quite large for both anisotropy models, but the ray solution with 10 higher-order approximations coincides with the exact solution quite well (within the width of the line).

6. Conclusion

Studying a simple problem of a plane S wave propagating in a weakly transversely isotropic medium with rotating axis of symmetry by ray theory, we have demonstrated that the S wave coupling ignored by zeroth-order ray theory (ZRT) can be successfully reproduced by higher-order ray theory (HRT). We have shown that ZRT can fail totally, while HRT yields the true solution. We have studied the accuracy of ray solution depending on number of the higher-order ray

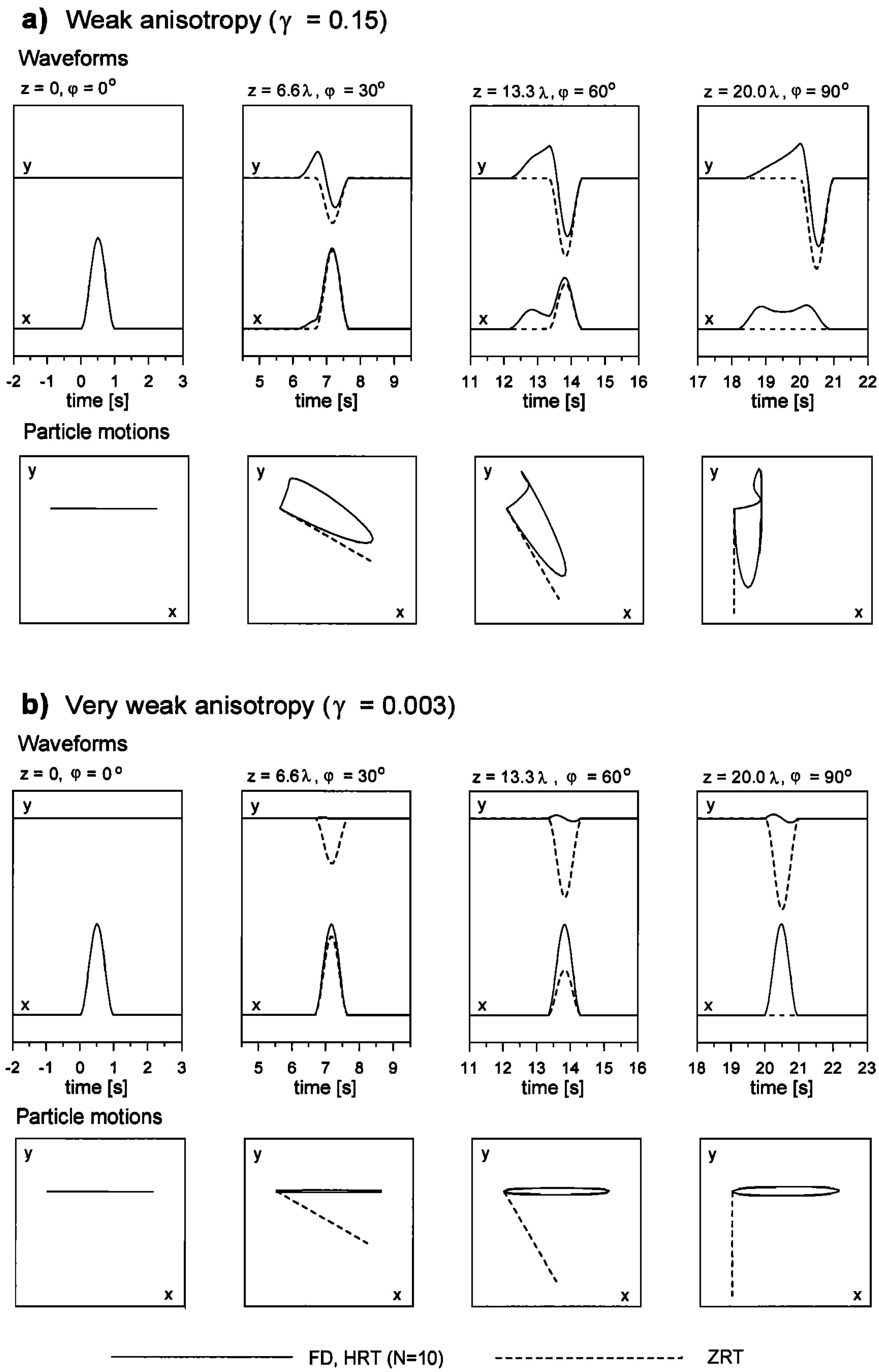

Figure 7. Waveforms and particle motions of the S wave propagating in (a) weak and (b) very weak anisotropy models. Diagrams are shown for four receivers with positions at z = 0, $6.6\lambda^{SR}$, $13.3\lambda^{SR}$, and $20.0\lambda^{SR}$, where λ^{SR} =2.45 km. The rate of rotation is $b = \varphi / z = \pi / 40\lambda^{SR}$ = 0.032. Solid line is FD solution and/or ray solution with 10 higher-order approximations. Dashed line is the ZRT solution.

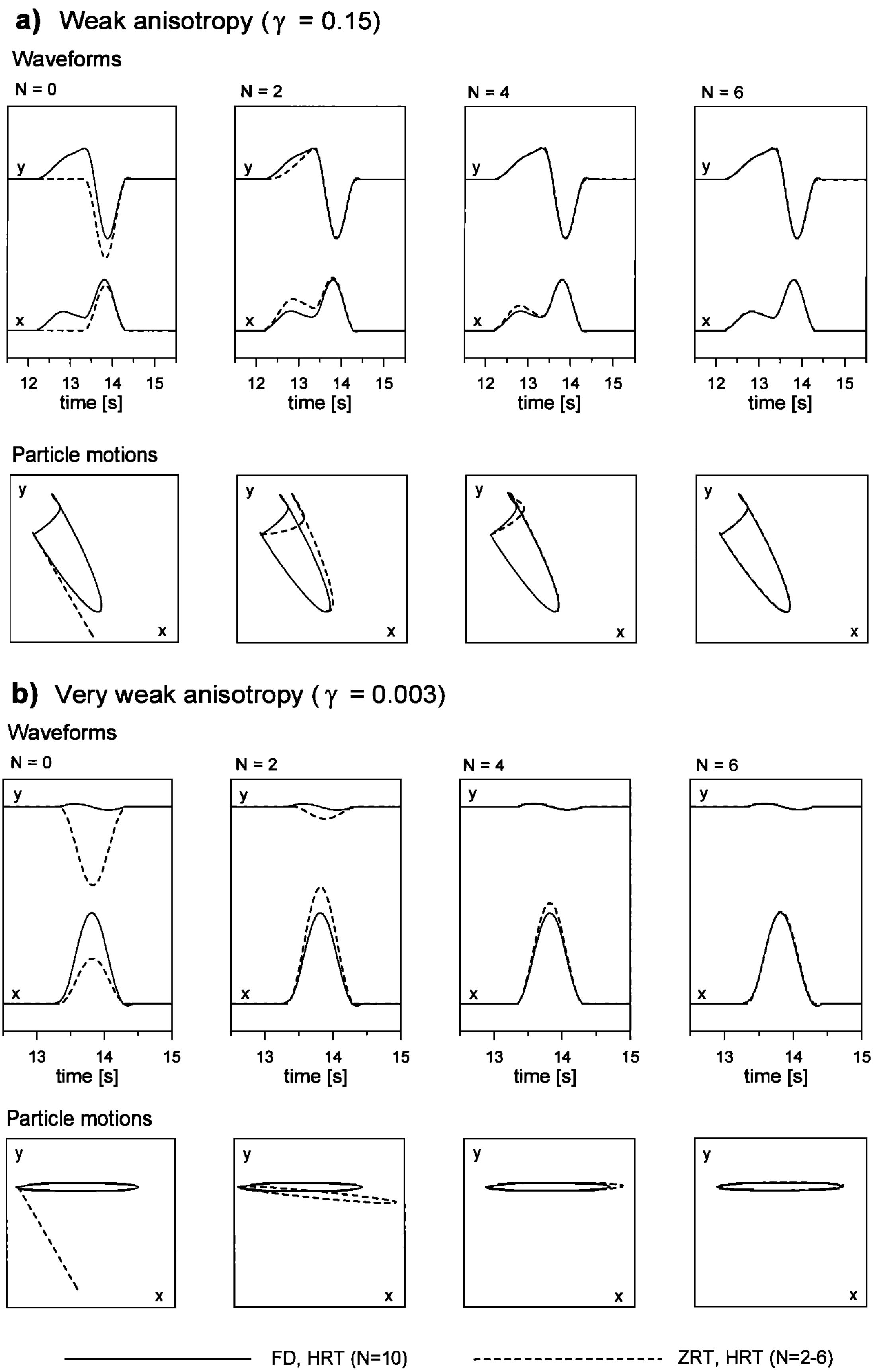

Figure 8. Waveforms and particle motions of the S wave propagating in (a) weak and (b) very weak anisotropy models. The receiver is at $z = 13.3\lambda^{SR}$ and the rate of rotation is $b = \pi/40\,\lambda^{SR} = 0.032$. Diagrams are shown for ray solutions with a different number of higher-order approximations: N = 0, 2, 4, and 6 (dashed line). Solid line is FD solution and/or ray solution with 10 higher-order approximations.

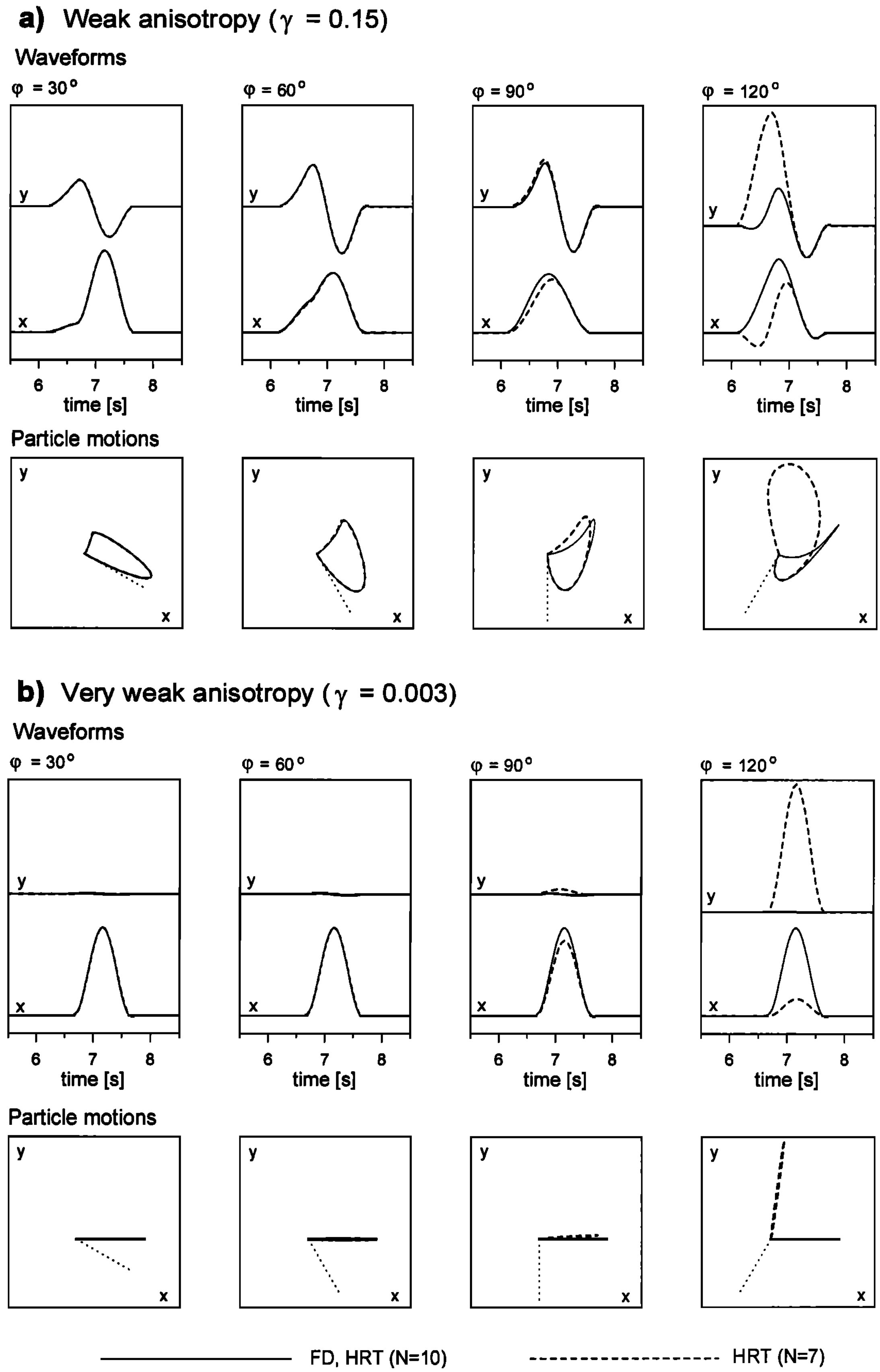

Figure 9. Waveforms and particle motions of the S wave propagating in (a) weak and (b) very weak anisotropy models. The receiver is at $z = 6.6\lambda^{SR}$. Diagrams are displayed for the rates of rotation (from left to right): $b = \pi / 40\, \lambda^{SR}$, $b = 2\pi / 40\, \lambda^{SR}$, $b = 3\pi / 40\, \lambda^{SR}$, and $b = 4\pi / 40\, \lambda^{SR}$. Solid line is FD solution and/or ray solution with 10 higher-order approximations. Dashed line is ray solution with seven higher-order approximations. Dotted line is projection of the symmetry axis into the x-y plane.

approximations considered, and we found that the accuracy increases with increasing number of higher-order ray approximations. This observation is valid even for very weak anisotropy almost approaching isotropy that is the most complicated case in ray theory. Furthermore, the accuracy decreases when the rate of rotation of the symmetry axis of the medium increases. For high values of the rate of rotation the elastic properties of the medium change significantly over distance comparable with the predominant wavelength of the propagating wave, and the basic condition for validity of ray theory is violated. Nevertheless, if we include a sufficient number of higher-order ray approximations, we can still obtain correct results. This implies that a condition of a large-scale inhomogeneity in a medium is not always an ultimate condition for the applicability of ray theory. We should stress, however, that for short-scale inhomogeneities the number of higher-order ray approximations having to be considered can be fairly high and thus computationally unrealizable even for a simple model. Finally, we observed that the accuracy of the ray solution decreases with increasing length of the ray of the propagating S wave. For more distant observers we have to include more terms of the ray series to obtain a comparable accuracy for all receivers.

The conclusions made for weak transverse isotropy are also valid for strong transverse isotropy if the S wave propagates near a kiss singularity. This occurs if the deviation between the rotating axis of symmetry and the vertical axis is small. If we limit this deviation to zero, the zeroth-order ray solution fails, but considering a sufficiently high number of higher-order ray approximations yields correct results.

Finally, we have to mention that we studied the S wave propagation in an extremely simple and in many aspects unrealistic structure. We did not discuss the aspects of computing the higher-order ray approximations in more realistic inhomogeneous anisotropic media. Therefore this paper should be viewed as a contribution to a general understanding of the problem of applicability of HRT rather than as an instruction how to apply HRT to modeling the S wave field in realistic situations. It can be expected that in many cases, when HRT works in principle, it need not to be practical or efficient or even possible to apply it in numerical computations. Nevertheless, it seems that further development of HRT, in particular, the development of its computing aspects, would be desirable.

Appendix A: Elastic Parameters of WTI With Rotating Axis of Symmetry

Elastic parameters a'_{kl} of the WTI medium with rotating axis of symmetry can be expressed by parameters a_{11}, a_{44}, and γ of the WTI medium with the vertical axis of symmetry (see equations (7) and (10)), by angle ϑ between the symmetry axis and the z axis, and by rotation angle φ as follows:

$$a'_{11} = a_{11}\,,\ a'_{22} = a_{11}\,,\ a'_{33} = a_{11}\,,$$

$$a'_{44} = a_{44}\left(1+2\gamma\sin^2\vartheta\cos^2\varphi\right)\ ,$$

$$a'_{55} = a_{44}\left(1+2\gamma\sin^2\vartheta\sin^2\varphi\right)\ ,$$

$$a'_{66} = a_{44}\left(1+2\gamma\cos^2\vartheta\right)\ ,$$

$$a'_{12} = a_{11} - 2a_{44}\left(1+2\gamma\cos^2\vartheta\right)\ ,$$

$$a'_{13} = a_{11} - 2a_{44}\left(1+2\gamma\sin^2\vartheta\sin^2\varphi\right)$$

$$a'_{14} = 4a_{44}\gamma\sin\vartheta\cos\vartheta\sin\varphi\ ,$$

$$a'_{23} = a_{11} - 2a_{44}\left(1+2\gamma\sin^2\vartheta\cos^2\varphi\right)\ ,$$

$$a'_{25} = -4a_{44}\gamma\sin\vartheta\cos\vartheta\cos\varphi\ ,$$

$$a'_{36} = -4a_{44}\gamma\sin^2\vartheta\sin\varphi\cos\varphi\ ,$$

$$a'_{45} = 2a_{44}\gamma\sin^2\vartheta\sin\varphi\cos\varphi\ ,$$

$$a'_{46} = 2a_{44}\gamma\sin\vartheta\cos\vartheta\cos\varphi\ ,$$

$$a'_{56} = -2a_{44}\gamma\sin\vartheta\cos\vartheta\sin\varphi\ ,$$

$$a'_{15} = 0\,,\ a'_{16} = 0\,,\ a'_{24} = 0\,,\ a'_{26} = 0\,,\ a'_{34} = 0\,,\ a'_{35} = 0\ .$$

Appendix B: Propagation of Plane S Waves Along the z Axis by Finite Differences (FD)

Since we are considering a vertically inhomogeneous medium in which a plane wave propagates along the z axis, displacement $\mathbf{u}$ will depend only on the z coordinate, $\mathbf{u} = \mathbf{u}(z,t)$. Equation (1) then simplifies to

$$\ddot{u}_1 - \left(a_{55}u_{1,3} + a_{45}u_{2,3}\right)_{,3} = 0\,,\ \ddot{u}_2 - \left(a_{45}u_{1,3} + a_{44}u_{2,3}\right)_{,3} = 0\,, \tag{B1}$$

$$\ddot{u}_3 - \left(a_{33}u_{3,3}\right)_{,3} = 0\ . \tag{B2}$$

Both (B1) and (B2) are independent. Equation (B1) represents a system of two coupled partial differential equations describing the propagation of plane S waves. Equation (B2) describes the propagation of a plane P wave. Since parameter a_{33} is constant (see Appendix A), the plane P wave behaves in the same way as in a homogeneous isotropic medium. Equation (B1) can be transformed into a system of four first-order partial differential equations

$$\dot{v}_1 = t_{1,3}\,,\ \ \dot{v}_2 = t_{2,3}\ , \tag{B3a}$$

$$\dot{t}_1 = a_{55}v_{1,3} + a_{45}v_{2,3}\,,\ \ \dot{t}_2 = a_{45}v_{1,3} + a_{44}v_{2,3}\,, \tag{B3b}$$

where v_1 and v_2 are the horizontal components of the particle velocity and t_1 and t_2 are components of the density-normalized stress tensor. We can write (B3) in a more compact matrix form as

$$\frac{d}{dt}\mathbf{y} = \mathbf{A}\frac{d}{dz}\mathbf{y}\,, \tag{B4}$$

where

$$\mathbf{A} = \begin{bmatrix} 0 & 0 & 1 & 0 \\ 0 & 0 & 0 & 1 \\ a_{55} & a_{45} & 0 & 0 \\ a_{45} & a_{44} & 0 & 0 \end{bmatrix},\quad \mathbf{y} = \begin{bmatrix} v_1 \\ v_2 \\ t_1 \\ t_2 \end{bmatrix}.$$

This equation is a time domain version of the matrix equation used by *Woodhouse* [1974, equation 2.9], *Fryer and Frazer*

[1984, equation 2.1] or *Chapman* [1994, equation 6], which is further simplified by considering the TI medium with a rotating axis of symmetry and by confining oneself only to the vertical direction of wave propagation.

Converting the derivatives in (B4) into finite differences by using the standard central difference formulae of second-order accuracy [*Aki and Richards*, 1980, p. 775] and using the explicit scheme, we obtain the system of FD equations in the following form:

$$\mathbf{y}(t+\Delta t,z)=\Delta t\left[\mathbf{A}\frac{\mathbf{y}(t,z+\Delta z)-\mathbf{y}(t,z-\Delta z)}{\Delta z}+\mathbf{y}(t-\Delta t,z)\right], \tag{B5}$$

where Δt and Δz are the time and space steps, which should satisfy the stability condition:

$$\Delta t \le \frac{\Delta z}{v^S}\ . \tag{B6}$$

Here v^S denotes the maximum value of the S wave group velocity. The size of the FD model is chosen in such a way that the studied wave field is not affected by the waves reflected from the boundary. Therefore we apply the simplest boundary conditions by specifying the rigid boundary. The S wave propagating in the model is initiated by applying the nonzero initial conditions at $z = 0$.

Acknowledgments. I thank Ivan Pšenčík for critically reading the manuscript and offering his comments and Luděk Klimeš for drawing my attention to the paper by *Lakhtakia* [1994]. I thank M. Kendall, G. Rümpker, and one anonymous reviewer for very helpful reviews. The work was supported by the Grant Agency of the Czech Republic, grant 205/96/0968, by the Consortium Project "Seismic waves in complex 3-D structures," and by the EC INCO-Copernicus Project IC15 CT96 200.

References

Aki, K., and P.G. Richards, *Quantitative Seismology. Theory and Methods* II, W. H. Freeman, San Francisco, 1980.

Červený, V., Seismic rays and ray intensities in inhomogeneous anisotropic media, *Geophys. J. R. Astron. Soc.*, *29*, 1-13, 1972.

Červený, V., I. Molotkov, and I. Pšenčík, *Ray Method in Seismogy*, Charles Univ. Press, Prague, 1977.

Chapman, C.H., Reflection/transmission coefficient reciprocities in anisotropic media, *Geophys. J. Int.*, *116*, 498-501, 1994.

Chapman, C.H., and P.M. Shearer, Ray tracing in azimuthally anisotropic media, II, Quasi-shear wave coupling, *Geophys. J.* , *96*, 65-83, 1989.

Coates, R.T., and C.H. Chapman, Quasi-shear wave coupling in weakly anisotropic 3-D media, *Geophys. J. Int.*, *103*, 301-320, 1990.

Crampin, S., Effects of point singularities on shear-wave propagation in sedimentary basins, *Geophys. J. Int.*, *107*, 531-543, 1991.

Fryer, G.J., and L.N. Frazer, Seismic waves in stratified anisotropic media, *Geophys. J. R. Astron. Soc.*, *78*, 691-710, 1984.

Guest, W.S., C.J. Thomson, and J-M. Kendall, Displacement and rays for splitting *S*-waves: Perturbation theory and the failure of the ray method, *Geophys. J. Int.*, *108*, 372-378, 1992.

Hearn, A.C., REDUCE 3.4. user's manual, RAND Corp., Santa Monica, Calif., 1991.

Lakhtakia, A., Elastodynamic wave propagation in a continuously twisted structurally chiral medium along the axis of spirality, *J. Acoust. Soc. Am.*, *95*, 597-600, 1994.

Pšenčík, I., Green functions for inhomogeneous weakly anisotropic media, *Geophys. J. Int.*, *135*, 279-288, 1998.

Rümpker, G., and P.G. Silver, Apparent shear-wave splitting parameters in the presence of vertically varying anisotropy, *Geophys. J. Int.*, *135*, 790-800, 1998.

Sharafutdinov, V.A., Quasi-isotropic approximation in dynamic elasticity and some problems of tomography, *Russian Geod. Geophys.*, *35*, 58-71, 1994.

Thomsen, L., Weak elastic anisotropy, *Geophysics*, *51*, 1954-1966, 1986.

Thomson, C.J., J.-M. Kendall, and W.S. Guest, Geometrical theory of shear-wave splitting: Corrections to ray theory for interference in isotropic/anisotropic transitions, *Geophys. J. Int.*, *108*, 339-363, 1992.

Vavryčuk, V., Elastodynamic and elastostatic Green tensors for homogeneous weak transversely isotropic media, *Geophys. J. Int.*, *130*, 786-800, 1997.

Vavryčuk, V., and K. Yomogida, *SH*-wave Green tensor for homogeneous transversely isotropic media by higher-order approximations in asymptotic ray theory, *Wave Motion*, *23*, 83-93, 1996.

Woodhouse, J.H., Surface waves in a laterally varying layered structure, *Geophys. J. R. Astron. Soc.*, *37*, 461-490, 1974.

Zillmer, M., B.M. Kashtan, and D. Gajewski, Quasi-isotropic approximation of anisotropic ray theory, *Geophys. J. Int.*, *132*, 643-653, 1998.

V.Vavryčuk, Geophysical Institute, Boční II/1401, 141 31 Praha 4, Czech Republic. (vv@ig.cas.cz)

(Received January 14, 1999; revised June 21, 1999;
accepted August 19, 1999)